



A late glacial – Holocene record of hydrological variability in Lake Baikal inferred from oxygen isotope analysis of diatom silica

Journal:	<i>Journal of Quaternary Science</i>
Manuscript ID:	JQS-10-0094
Wiley - Manuscript type:	Research Article
Date Submitted by the Author:	22-Jun-2010
Complete List of Authors:	Mackay, Anson; UCL, Geography Swann, George; NERC Isotope Geosciences Laboratory Brewer, Tim; University of Leicester, Department of Geology Leng, Melanie; NERC Isotope Geosciences Laboratory Morley, David; UCL, Department of Geography Piotrowska, Natalia; Silesian University of Technology, Department of Radioisotopes Rioual, Patrick; Chinese Academy of Science, Geology and Geophysics Institute White, Dustin; University of Oxford, Institute of Archaeology
Keywords:	Lake Baikal, $\delta^{18}\text{O}$ diatom, late glacial, Holocene, IRD events



1
2
3
4
5
6
7
8
9
10
11
12
13
14
15
16
17
18
19
20
21
22
23
24
25
26
27
28
29
30
31
32
33
34
35
36
37
38
39
40
41
42
43
44
45
46
47
48
49
50
51
52
53
54
55
56
57
58
59
60

1
2
3
4
5
6
7
8
9
10
11
12
13
14
15
16
17
18
19
20
21
22
23
24
25
26
27
28
29
30
31
32
33
34
35
36
37
38
39
40
41
42

A late glacial – Holocene record of hydrological variability in Lake Baikal inferred from oxygen isotope analysis of diatom silica.

Anson W. Mackay^{a,1}

^aEnvironmental Change Research Centre, Department of Geography, UCL, Gower Street London. United Kingdom. WC1E 6BT.

Email: a.mackay@ucl.ac.uk

¹Corresponding author

George E.A. Swann^b

^bNERC Isotope Geosciences Laboratory, British Geological Survey, Keyworth, Nottingham, NG12 5GG, UK

Tim S. Brewer^{c,2}

^cDepartment of Geology, University of Leicester, Leicester, United Kingdom. LE1 7RH.

²Deceased

Melanie J. Leng^{b,d}

^bNERC Isotope Geosciences Laboratory, British Geological Survey, Keyworth, Nottingham, NG12 5GG, UK

^cSchool of Geography, University of Nottingham, Nottingham, United Kingdom. NG7 2RD

David W. Morley^{a,e}

^aEnvironmental Change Research Centre, Department of Geography, UCL, Gower Street London. WC1E 6BT

^e Spatial Ecology and Epidemiology Group, Department of Zoology, South Parks Road, University of Oxford, Oxford, United Kingdom. OX1 3PS

Natalia Piotrowska^f

^fSilesian University of Technology, Institute of Physics, Department of Radioisotopes, GADAM Centre of Excellence, Krzywoustego 2, 44-100 Gliwice, Poland

Patrick Rioual^g

^gGeology and Geophysics Institute, Chinese Academy of Science, P.O. Box 9825, Beijing 100029, China

Dustin White^h

^hInstitute of Archaeology, University of Oxford, 36 Beaumont Street, Oxford, United Kingdom. OX1 2PG.

Abstract

Here we present a new palaeoenvironmental record of hydrological variability in Lake Baikal since c. 14 100 cal yrs BP, based on re-modelled $\delta^{18}\text{O}_{\text{diatom}}$ values of diatom silica ($\delta^{18}\text{O}_{\text{modelled}}$), where the residual contaminants are identified and compensated for using electron optical imaging and whole sample geochemistry. $\delta^{18}\text{O}_{\text{modelled}}$ interpretations are based on the balance between isotopically higher rivers, which have catchments to the south of Lake Baikal, and isotopically lower rivers with catchments to the north. Isotopic differences are due to varying proportions of precipitation and snow-melt which feed these rivers. The balance between northern and southern rivers flowing into Lake Baikal is mediated by the strength of the Siberian High. Overall, episodic declines in $\delta^{18}\text{O}_{\text{modelled}}$ values show good agreement with increases in %HSG grains in the North Atlantic (indicative of ice-rafted debris events). Periods when the contribution of isotopically lower rivers with northern catchments increases are coincident with increases with IRD events at e.g. c. 11 300 cal yr BP (IRD8), c. 10 200 cal yr BP (IRD7), c. 8 400 cal yrs BP (IRD5), c. 7 000 cal yrs BP, c. 5 900 cal yrs BP (IRD4) and 3 330 cal yrs BP (IRD2). Isotopically higher input from rivers to the south Lake Baikal is especially dominant between c. 3 300 – 2 000 cal yrs BP, concurrent with high precipitation amounts in the Lake Baikal region and northern Mongolia. This study highlights the potential for oxygen isotope analysis of diatom silica to reconstruct the past hydrology of Lake Baikal, and its possible relationship with distant events such as changes in the North Atlantic thermohaline circulation.

Keywords: Lake Baikal; $\delta^{18}\text{O}_{\text{diatom}}$; late glacial; Holocene; IRD events

1. Introduction

Lake Baikal (51°28' - 55°47' N and 103°43' - 109°58' E) in central Asia is situated in one of the most continental regions of Earth, where climate is strongly influenced the Siberian High, a high pressure cell which starts to build in strength in August, and remains strong until the following April. Precipitation to the Lake Baikal region mainly originates from the North Atlantic and is transported via the Westerlies (Lydolph 1977; Numaguti 1999; Kurita et al. 2004), with very little contribution from tropical sources (Sato et al. 2007). Precipitation throughout the Lake Baikal region is greatest during June, July and August (JJA) (Kozhova & Izmet'eva 1998). Winters on the other hand are dominated by the Siberian High, which ensures that winters are cold, dry and long (Lydolph 1977). Lake Baikal contains approximately one fifth of the world's global resources of surface freshwater, and species living in the lake exhibit high levels of endemism (Kozhova & Izmet'eva 1998). Given recent debates on threats to freshwater resources and biodiversity, understanding the functioning of such a complex ecosystem remains an important research priority. Climate is a major driver of ecosystem change, and studies have demonstrated the impacts of recent warming on both the ice cover of Lake Baikal (e.g. Livingstone 1999; Todd & Mackay 2003) and on its biology (Mackay et al. 2005; Hampton et al. 2008). To gain a wider perspective on these changes, it is important to study hydrological trends in Lake Baikal over longer timescales.

1 For example, during the late glacial, one of the most distinctive shifts in climate was the
2 period commonly known as the Younger Dryas (GS-1), c. 12 900 cal yrs BP. This abrupt
3 cold reversal in the North Atlantic region is linked to an enormous pulse of freshwater
4 being released from the Laurentide ice sheet into the Arctic Ocean (Tarasov and Peltier
5 2005; Murton et al., 2010), causing a decline in global temperatures (as inferred from
6 $\delta^{18}\text{O}$ records from the Greenland ice cores). During the Holocene, centennial-scale cool
7 events (Bond events (Bond et al. 1997)) have been identified in natural archives from
8 around the world (e.g. Campbell et al. 1998; deMenocal et al. 2000; Heiri et al. 2004;
9 Mayewski et al. 2004; Nesje et al. 2005; Wanner et al. 2008). These events are associated
10 with pulses of freshwater discharge from the Laurentide ice sheet weakening North
11 Atlantic thermohaline circulation (THC), resulting in the southwards extension of polar
12 waters (Bond et al. 1997). Changes in solar insolation are also implicated (e.g. Bond et al.
13 2001), whilst after c. 8 000 cal yrs BP these events are likely due to a combination of
14 other factors (Wanner et al. 2008).

15
16 In dilute, lacustrine systems where preservation of carbonates is poor (such as Lake
17 Baikal), oxygen isotope analysis of diatom silica ($\delta^{18}\text{O}_{\text{diatom}}$) is potentially an important
18 palaeoclimatic technique that can be used as a direct replacement for $\delta^{18}\text{O}$ from
19 carbonates. For example, during the last glacial – interglacial transition in southwest
20 Alaska, a decline in $\delta^{18}\text{O}_{\text{diatom}}$ values at the start of the Younger Dryas was interpreted as
21 being caused by a drop in temperature of over 3.5 °C (Hu & Shemesh 2003). In Lake 850,
22 close to Abisko in the Swedish Arctic, $\delta^{18}\text{O}_{\text{diatom}}$ values are thought to reflect varying
23 sources of precipitation to the region, such that a persistent decline in $\delta^{18}\text{O}_{\text{diatom}}$ during
24 the Holocene is linked to increasing influence of the polar Arctic continental air mass
25 (Shemesh et al. 2001). Through $\delta^{18}\text{O}_{\text{diatom}}$ analyses of lake sediments from the Kola
26 Peninsula, polar Arctic air masses were also shown to dominate this region of northwest
27 Russia during the early and late Holocene, while during the mid Holocene maritime
28 Atlantic air masses were important (Jones et al. 2004). In a further study of a proglacial
29 lake in the Swedish Arctic, Rosqvist et al. (2004) demonstrate a clear correlation between
30 periods of glacier advancement and $\delta^{18}\text{O}_{\text{diatom}}$ minima during the late Holocene linked to
31 increased influence of polar air masses. These minima occur at approximately the same
32 time as Bond events, confirming the increased influence of N-NE winds in this region of
33 the north Atlantic (Rosqvist et al. 2004).

34
35 $\delta^{18}\text{O}_{\text{diatom}}$ analyses have previously been used to reconstruct environmental change in
36 Lake Baikal during the late glacial (Morley et al. 2005), MIS 3-1 (Kalmychkov et al.,
37 2007) and during MIS 11 (Mackay et al. 2008). In Lake Baikal, changes in $\delta^{18}\text{O}_{\text{diatom}}$
38 values have been linked to variation in fluvial input, most notably between rivers with
39 catchments which extend to the south of Lake Baikal into Mongolia, with rivers with
40 more northerly catchments (Fig 1). Changes in air temperature have been considered, but
41 given that rainfall water–temperature fractionation is +0.36‰/°C (the Dansgaard
42 temperature dependence in precipitation at Irkutsk), shifts in isotopic values observed in
43 Lake Baikal records are too great to have been caused by temperature alone (Seal and
44 Shanks 1998; Morley et al. 2005). Over 330 rivers flow into Lake Baikal, the most
45 significant being the Selenga, Upper Angara and Barguzin Rivers contributing c. 50%,
46 14% and 7% of total annual river inflow respectively (Shimaraev et al. 1994) (Fig. 1).

1 The Selenga River therefore is by far the most important river in terms of hydrological
2 input into Lake Baikal. Just under half of Lake Baikal's catchment belongs to the Selenga
3 River basin, c. 280,000 km², which drains much of northern Mongolia between 46-52° N
4 and 96-109° E (Fig. 1) (Ma et al. 2003). Any changes in its flow therefore will result in
5 hydrological changes in the lake itself.

6
7 Lake Baikal contains three large basins (north, central, south) and the form of moisture
8 contributing to river flow to these basins varies considerably. For example, snow-derived
9 water accounts for just under one third of total fluvial input into the north basin. The
10 Selenga River on the other hand, which drains into the south and central basins, consists
11 of only c. 15% snow-derived water (Afanasjev 1976). Conversely, the proportion of water
12 derived from rainfall is highest in the Selenga River (almost 40%), whereas for rivers that
13 flow into the north basin, this proportion drops to only c. 20%. These contribute to the
14 variation in isotope values of modern waters which show that rivers with catchments to
15 the south of Lake Baikal are characterized by higher $\delta^{18}\text{O}$ values (e.g. -13.5‰ for the
16 Selenga River), in comparison to rivers with more northern catchments (e.g. the Barguzin
17 and Upper Angara Rivers) with lower $\delta^{18}\text{O}$ values (-17.3‰ and -19.8‰ respectively;
18 Seal and Shanks 1998). During periods of cooler temperatures and prolonged winters,
19 instrumental and remotely sensed data show that increased Eurasian spring snow cover
20 extent results in a reduction in summer precipitation (especially over the Selenga
21 catchment) through increased anticyclonic activity and strength of the Siberian High (Lui
22 & Yanai 2002). Thus rivers with higher $\delta^{18}\text{O}$ values to the south of Lake Baikal decline in
23 volume, while northern rivers fed by a higher proportion of snowmelt increase (Morley et
24 al. 2005). Previous work investigating trends in ice cover on Lake Baikal has shown
25 significant links with northern annular modes (especially the North Atlantic Oscillation
26 and Arctic Oscillation; Livingstone 1999; Todd & Mackay 2003). It is possible that these
27 modes are also having an impact on transport of moisture to the Lake Baikal region via
28 the Westerlies.

29
30 Demske et al. (2005) suggested that there is distinct pollen evidence for climatic impact
31 in the Lake Baikal region related to Holocene cool events in the North Atlantic (Bond et
32 al. 1997). A major aim of this paper therefore, is to assess any potential impact of such
33 cool events on hydrological inflow into Lake Baikal. In order to do this, we present a new
34 $\delta^{18}\text{O}_{\text{diatom}}$ record derived from the recalculation of data first published by Morley et al.
35 (2005). This recalculation is necessary due to recent advances in the application of whole
36 sample geochemistry coupled with electron-optical imaging in providing a method for the
37 identification, estimation and subsequent removal of the effects of clay and silt
38 contamination on $\delta^{18}\text{O}_{\text{diatom}}$ data (Brewer et al. 2008). Due to issues of contamination on
39 the $\delta^{18}\text{O}_{\text{diatom}}$ record by silts and clays, palaeo-environmental interpretations of the
40 Holocene were barely made by Morley et al. (2005). We also take advantage of IntCal04
41 calibration curve over IntCal98, which provides much improved calibrated dates for
42 samples deposited prior to 11 400 cal yrs BP, a key timeframe in our analyses (Blackwell
43 et al. 2006).

44 45 **3. Materials and methods**

46

3.1 Site location and coring

The Vydrino Shoulder (51.58°N, 104.85°E) is located off the southeastern coast of Lake Baikal (c. 5 km) between 500 – 800 m water depth (Fig. 1). Given its proximity to the shore, Vydrino is also likely influenced by fluvial input from nearby rivers, including the Snezhnaya and Vydrinaya. The Shoulder forms an upper- to mid-slope terrace dissected by several canyons (Charlet et al. 2005) and is in the vicinity of several underwater channels. In the summer of 2001, different core types of varying length were extracted from a ridge location (>600 m water depth) on the Vydrino Shoulder. Of relevance to this study, these include a long piston core over 10 m in length and a separate box core of c. 2.5 m in length (Table 1). This ridge was selected because seismic profiling and side-scan sonar analyses revealed a stable area of fine-grained sedimentation relatively undisturbed by tectonic activity and reworking (Fig. 3 in Charlet et al. 2005).

3.2 Chronology

Plant macrofossils are rarely preserved in the pelagic sediments of Lake Baikal, so AMS ^{14}C dates were obtained from pollen and spore concentrates (Piotrowska et al. 2004; Demske et al. 2005). The late glacial – Holocene age model for Vydrino Shoulder is based upon twelve AMS ^{14}C pollen dates from the box core (CON01-605-5) (Piotrowska et al. 2004) and an additional five AMS ^{14}C pollen dates from the piston core (CON01-605-3) (Demske et al. 2005). Pollen purity was excellent (80% – 95%) in each box-core sample due to the presence of very high concentrations of large bisaccate pollen grains (Table 2); unfortunately purity data for the pollen extracts obtained from the piston cores are not available, which indirectly adds to uncertainty of dates obtained for pre-Holocene sediments. Dates from the box core were transferred to the piston core based on easily identified peaks in relative abundances of specific diatom species common to both cores, including a well defined peak of *Hannaea baicalensis* Genkal, Popovskaya, Kulikovskiy during the early Holocene, and a mid Holocene switch between *Crateriportula inconspicua* and *Synedra acus* (Kützing) (data not shown - see Morley 2005 and Morley et al. 2005). All radiocarbon dates were calibrated using OxCal 4.1 program (Bronk Ramsey 2009) and IntCal04 radiocarbon calibration curve (Reimer et al. 2004) (Table 2). To estimate a relationship between age and depth we used a generalised mixed-effect regression based on a generalised additive model (GAM) with constant variance (Heegaard et al. 2005).

3.3 $\delta^{18}\text{O}_{\text{diatom}}$ analysis

Samples for $\delta^{18}\text{O}_{\text{diatom}}$ came from the piston core (CON01-605-3). Sediments were originally analysed for $\delta^{18}\text{O}_{\text{diatom}}$ at contiguous 2 cm intervals by Morley et al. (2005), although a reduced dataset is presented here. The methodology for cleaning samples for $\delta^{18}\text{O}_{\text{diatom}}$ analysis has previously been reported by Morley et al. (2004), and involves the step-wise removal of contaminants using chemical and physical separation techniques. Cleaned, dried samples were first subjected to a prefluorination process to remove the unstable hydrous silica layer from the diatom valves, before full reaction with BrF_5 (Leng and Sloane, 2008). Liberated oxygen was converted to CO_2 and measured alongside BFC_{mod} the NIGL diatom standard with $\delta^{18}\text{O}$ analysis performed using an Optima dual inlet mass spectrometer. The data are presented as per mil (‰) deviations from SMOW

1 with replicate analysis of sample material indicating an analytical reproducibility of
2 $\pm 0.34\%$ (1 σ).

3
4 Subsequent SEM analyses of these cleaned samples demonstrated that a small but
5 significant proportion of contaminants remained after sample preparation. These
6 contaminants were comprised of clay and silt material trapped, for example, within the
7 cylindrical frustules of *Aulacoseira* species or as clay particles coated with sub-micron
8 scale diatom fragments (Brewer et al. 2008). Morley et al. (2005) tried to compensate for
9 these remaining contaminants by calculating the $\delta^{18}\text{O}$ value of the non-diatom particles as
10 an average of clay and silt sized mineral/rock grains (called 'silt') remaining in the
11 sample following the removal of diatoms with sodium hydroxide ($12.3 \pm 1.8\%$, 2 S.D.,
12 $n=3$). A mass balanced $\delta^{18}\text{O}$ value for pure diatoms ($\delta^{18}\text{O}_{\text{modelled}}$) was therefore calculated
13 using the estimated percentage content of diatoms and silt identified using light
14 microscopy for individual samples. This methodology however underestimates the effect
15 of silt $\delta^{18}\text{O}$ because volumes of diatoms and silt particles are not taken into account (Leng
16 and Barker 2006), resulting in a significant uncertainty in the original $\delta^{18}\text{O}_{\text{modelled}}$ data.
17 Due to this, an interpretation of the Holocene $\delta^{18}\text{O}_{\text{diatom}}$ and $\delta^{18}\text{O}_{\text{modelled}}$ record was barely
18 made (Morley et al. 2005).

19
20 This study differs significantly from Morley et al. (2005) because we use a mass-balance
21 approach where the residual contaminants are identified and compensated for, using
22 electron optical imaging and whole sample geochemistry (see Brewer et al. 2008 for full
23 methodological details). Note however, that only 55 of the 130 samples analysed by
24 Morley et al., (2005) contained sufficient quantities of diatoms for XRF analysis,
25 resulting in a substantial reduction in sample resolution. Under the geochemical mass
26 balancing approach, the relative amount of silt contamination can be calculated from the
27 amount of Al_2O_3 in individual samples. Brewer et al., (2008) achieved this by:

$$\% \text{silt} = (\text{sample}_{\text{Al}} / \text{silt}_{\text{Al}}) \times 100 \quad (1)$$

29
30 where $\text{sample}_{\text{Al}}$ is the measured Al_2O_3 concentration in each sample analysed for
31 $\delta^{18}\text{O}_{\text{diatom}}$ and silt_{Al} the average $\% \text{Al}_2\text{O}_3$ in the Baikal silt sample, calculated in Brewer et
32 al (2008) as 16.8%.

33
34 A key assumption of this is that concentrations of Al within diatoms are negligible. A
35 number of studies, however, have shown that fossilised diatoms can contain up to 1 wt.%
36 Al (see Koning et al. (2007) and references within). Recent work on fully purified MIS 5e
37 diatom samples from Lake Baikal shows Al concentrations of 0.08% [$1\sigma = 0.02$] (Swann
38 in press). Although this level of diatom bound Al typically only alters modelled $\delta^{18}\text{O}_{\text{diatom}}$
39 within the limits of analytical reproducibility (0.34%) it nevertheless remains important
40 to account for this contribution. By assuming that Al concentrations in MIS 5e diatoms
41 from Lake Baikal are representative of the late glacial – Holocene aged diatoms analysed
42 here, a separate initial mass balance calculation can be performed to distinguish between
43 diatom Al/silt Al and so calculate $\% \text{diatom}$ and $\% \text{silt}$:

$$\text{sample}_{\text{Al}} = (\% \text{diatom} \cdot \text{diatom}_{\text{Al}}) + (\% \text{silt} \cdot \text{silt}_{\text{Al}}) = (\% \text{diatom} \cdot 0.15) + (\% \text{silt} \cdot 17.2\%) \quad (2)$$

where $\text{diatom}_{\text{Al}}$ is the %Al in diatom converted into %Al₂O₃, %diatom and %silt the percent diatom and silt within the analysed sample and silt_{Al} is the corresponding value from Brewer et al (2008) re-normalised following the removal of LOI data which constitutes water and other organic matter that will be removed during the pre-fluorination stage of the $\delta^{18}\text{O}_{\text{diatom}}$ analysis. A further mass balance correction is then employed to account for the effects of silt contamination on the measured $\delta^{18}\text{O}$ values:

$$\delta^{18}\text{O}_{\text{modelled}} = (\delta^{18}\text{O}_{\text{diatom}} - \% \text{silt}_\text{O}/100 \times \delta^{18}\text{O}_{\text{silt}})/(\% \text{diatom}_\text{O}/100) \quad (3)$$

where $\delta^{18}\text{O}_{\text{modelled}}$ is the mass balance corrected value of $\delta^{18}\text{O}_{\text{diatom}}$, $\delta^{18}\text{O}_{\text{diatom}}$ is the original isotope value of the “cleaned” diatom sample, $\delta^{18}\text{O}_{\text{silt}}$ is the average isotope value of silt from Lake Baikal, measured at $11.7 \pm 0.3\text{‰}$ (n=6) in Brewer et al. (2008), and $\% \text{diatom}_\text{O}/\% \text{silt}_\text{O}$ is the percentage of diatom and silt with respect to oxygen. $\% \text{silt}_\text{O}$ is calculated by assuming that 48.6 wt.% of the contaminant silt is comprised of oxygen (c.f., Brewer et al., 2008) whilst for $\% \text{diatom}_\text{O}$ we assume that diatoms are comprised of SiO₂ with oxygen making up 53.3% of the diatom frustule. An estimate of the error associated with this mass balance correction can be obtained for each sample by factoring in an analytical reproducibility of 0.34‰ for both the diatom and Baikal silt isotope measurements into equation 3.

4. Results and Discussion

The calibrated ages for our profile span approximately the last 15 700 cal yrs BP (range 15 275 – 16 090 cal yrs BP) (Fig 2). The age-depth curve was determined using mixed-effect regression (Heegaard et al. 2005). The calculations of model confidence intervals take into consideration not only the width of probability distribution of calibrated ages, but also the representativity of individual dates for the sequence. The average 95% confidence intervals for most of the profile (13 000 – 2 000 cal yrs BP) range from ± 120 to ± 200 years. For the younger part, the confidence intervals increase from ± 35 to ± 150 years, while for the ages older than 13 000 cal yrs BP they continuously rise from ± 200 to almost ± 400 years. As the thickness of the sediment samples used for dating is taken into account, this results in the wider confidence intervals observed during the late glacial, early Holocene period (see Table 2). The model also reveals that the top-most radiocarbon date is not close to the expected value, and therefore probably poorly represents the real age of this layer (Heegaard et al. 2005). Given this chronology, the resolution of the $\delta^{18}\text{O}_{\text{modelled}}$ profile varies between c. 375 – 400 years. Using the IntCal04 calibration curve, the timing of $\delta^{18}\text{O}_{\text{modelled}}$ changes during the early part of our record have changed substantially from that first presented by Morley et al. (2005) by c. 1000 years. For example, the low $\delta^{18}\text{O}_{\text{diatom}}$ value reported by Morley et al. (2005) at c. 11 300 cal yrs BP is estimated now to occur at c. 10 300 cal yrs BP, which is a direct result of the improved calibration curve during this key period (Blackwell et al 2006).

Robust interpretations of $\delta^{18}\text{O}_{\text{diatom}}$ data from lake sediments are reliant on intensive cleaning and mass balance modelling procedures for removing effects of contaminants. Brewer et al. (2008) showed that Baikal silt is enriched in Al₂O₃, Fe₂O₃, Na₂O and K₂O,

1 such that the incorporation of silt within diatom samples should be clearly identifiable
2 through their trace element geochemistry. Using sample Al_2O_3 concentrations as an
3 estimator of contamination, the amount of non-diatom material within the Vydrino
4 samples ranges from <10% to c. 90%. This highlights that the purification method
5 described by Morley et al. (2004) can be inefficient. The presence of non-diatom
6 contaminants in samples analysed for $\delta^{18}\text{O}_{\text{diatom}}$ or other diatom isotopes/geochemical
7 analyses is not restricted to Lake Baikal. Regardless of the adopted procedure, the
8 majority of lacustrine and marine samples will contain a proportion of clays, silts, or
9 other siliceous material such as sponges or phytoliths after sample cleaning (Leng and
10 Barker, 2006; Lamb et al., 2007; Swann and Leng, 2009). Indeed some samples are
11 impossible to fully purify due to contaminants becoming electro-statically charged to
12 frustules (Brewer et al, 2008). Despite this, in the majority of cases issues of
13 contamination are not considered despite their potential to distort the isotope record.
14 Increasing awareness of these issues and the development of more sophisticated methods
15 for assessing levels of contamination are however beginning to resolve this issue (Swann
16 and Leng, 2009). The mass balanced $\delta^{18}\text{O}_{\text{modelled}}$ data presented here therefore are a re-
17 analysis of a subset of data previously presented by Morley et al. (2005), but with
18 significant and important modifications. First, we are able to attribute error estimates to
19 each modelled $\delta^{18}\text{O}$ value. Second, modelled $\delta^{18}\text{O}$ values have some of the high-
20 frequency noise and some of the large low-frequency excursions removed (Fig 3). For
21 example, mean $\delta^{18}\text{O}_{\text{modelled}}$ values are c. 5‰ higher using the mass-balance approach,
22 with considerably smaller standard deviation (Table 3). Most striking is the influence of
23 silt contamination on the records. The original record by Morley et al. (2005) is strongly
24 influenced by the proportion of silt in the sample, such that as %silt increases, $\delta^{18}\text{O}_{\text{diatom}}$
25 values decline, in line with lower $\delta^{18}\text{O}$ value for silt. However, our $\delta^{18}\text{O}_{\text{modelled}}$ values
26 exhibit a very different response with the contamination record; during the early
27 Holocene, $\delta^{18}\text{O}_{\text{modelled}}$ values increase as silt contamination increases, and again to a
28 lesser extent during the mid Holocene (Fig 3). Other potential confounding factors such
29 as dissolution and vital effects for Lake Baikal diatoms are considered in detail in
30 Mackay et al. (2008).

31 32 **4.1 Palaeo-environmental interpretations**

33 34 4.1.1 The late glacial period

35
36 The Bølling interstadial was the first period of warming after the last glacial, and is dated
37 to approximately 14 600 – 14 100 cal yrs BP. $\delta^{18}\text{O}_{\text{modelled}}$ values are relatively high (c.
38 +28‰) at this time, indicative of rivers such as the Selenga, with catchments to the south
39 of Lake Baikal, dominating fluvial input. This is in line with a two-fold increase in
40 precipitation, which resulted in increased catchment weathering around Lake Baikal,
41 through increased river inflow and reduced aeolian transport (Chebykin et al. 2002). In
42 the catchment, warming is associated with a marked expansion in shrub landscape,
43 especially *Salix* species and *Alnus fruticosa* (Demske et al. 2005). Thus, although
44 prevailing humidity and precipitation had increased, temperatures were still relatively
45 cool, because *A. fruticosa* is characteristic of the sub-alpine mountain zone around Lake
46 Baikal today. Two other diatom records from Lake Baikal also show moderate increases

1
2
3 1 in diatom concentration during the Bølling period (Prokopenko et al. 2007). During the
4 2 Allerød, the $\delta^{18}\text{O}_{\text{modelled}}$ record exhibits a low value of +25.3‰ at c. 13 450 cal yrs BP
5 3 (Fig. 4), coincident with a decline in diatom concentration reported by Prokopenko et al.
6 4 (2007) at c. 13 500 cal yrs BP. However, this decline in the isotope record is characterised
7 5 by one point only, and future higher resolution work is needed to determine if this is a
8 6 real shift in balance from rivers flowing into Lake Baikal from the south, to isotopically
9 7 lower rivers flowing in from the north, associated with the timing of the onset of the
10 8 intra-Allerød cold period (IACP) (e.g. Rasmussen et al. 2006).
11 9

12 10 The transition from the Allerød into the Younger Dryas is generally placed at c. 12 900
13 11 cal yrs BP. Proxy records in Lake Baikal are indicative of a decline in primary
14 12 productivity with the onset of the Younger Dryas, although moisture records appear to be
15 13 more complex. For example, a coarsely resolved biogenic silica record from BDP93
16 14 (Buguldeika Saddle) demonstrated a decline in diatom productivity linked to the Younger
17 15 Dryas (Colman et al. 1999) while pigments such as total chlorophyll *a* from BDP93 also
18 16 declined (Soma et al. 2007). Corresponding diatom concentrations from BDP93 also
19 17 show a small reduction at this time, followed by a small increase at c. 12 000 cal yrs BP
20 18 (Prokopenko et al. 2007). More recently, Watanabe et al. (2009) showed that between 12
21 19 800 – 11 600 cal yrs BP, mass accumulation rates of total organic carbon (MAR_{TOC}) on
22 20 the Academician Ridge rapidly declined, indicative of falling productivity in the lake
23 21 together with a decline in terrestrial organic material. At the start of the Younger Dryas
24 22 $\delta^{18}\text{O}_{\text{modelled}}$ values initially decline to c. +26.9‰ indicative of only a small decline in river
25 23 inflow into the south basin of Lake Baikal which persisted til c. 12 180 cal yrs BP. Pollen
26 24 reconstructions show that by c. 12 500 cal yrs BP although temperatures dropped, low
27 25 levels of evaporation maintained a rather humid climate (Tarasov et al. 2007). Pollen
28 26 evidence elsewhere suggests that regions of peat formation around Lake Baikal started at
29 27 the Allerød - Younger Dryas transition, again indicative that any decline in precipitation
30 28 during the Younger Dryas was not enough to halt peat accumulation (Bezrukova et al.
31 29 2005). Further afield, detailed investigations on the palaeohydrology of Lake Hovsgol,
32 30 which lies in the catchment of Lake Baikal, demonstrate that lake levels there started to
33 31 increase irreversibly by about 15 400 cal yrs BP, which Prokopenko et al. (2005, 2009)
34 32 suggest is due to increased precipitation in the southern catchment of Lake Baikal, before
35 33 the start of the Holocene period. Further evidence for complex climate patterns during the
36 34 Younger Dryas in this region of central Asia comes from Quaternary lake-level
37 35 fluctuations of two northern Mongolian lakes (Bayan Nuur and Uvs Nuur) which exhibit
38 36 high lake level stands from the Allerød through to the early Holocene, linked to melting
39 37 glaciers and increased precipitation (Grunert et al. 2000). Increasing $\delta^{18}\text{O}_{\text{modelled}}$ values
40 38 from c. 12 180 cal yrs BP suggest increased Westerly transport of precipitation to rivers to
41 39 the south Lake Baikal, which must have been accompanied by a decline in intensity of
42 40 the Siberian High. These findings are line with increasing pollen-inferred precipitation by
43 41 c. 12 000 cal yrs BP elsewhere in the Lake Baikal region (Tarasov et al. 2009), and
44 42 increasing global temperatures by c. 12 000 cal yrs BP (Stuiver et al. 1995). Overall,
45 43 evidence from different proxies in the Lake Baikal region point to a period of reduced
46 44 productivity but sustained effective moisture during the early stages of the Younger
47 45 Dryas. By about 12 000 cal yrs BP however, hydrological inflow from isotopically higher
48 46 rivers to the south of the lake increased again.
49
50
51
52
53
54
55
56
57
58
59
60

4.1.2 Early - mid Holocene (11 700 – 7 000 cal yrs BP)

We define the early Holocene as being the period when ice sheets were still a significant feature of northern hemisphere landscapes, modulating a climate which was principally being driven by orbital parameters. Relative summer insolation values at temperate latitudes (e.g. 53° N) were at their highest during the early Holocene, c. 10 000 cal yrs BP before gradually declining to the present day (Prokopenko et al. 2007). Average annual temperatures during the early Holocene were progressively getting warmer, although in central Asia, the difference between seasonal temperatures at temperate latitudes was very pronounced because of high obliquity resulting in relatively warm summers but very cold winters (Bush 2005). Here we show alongside the $\delta^{18}\text{O}_{\text{modelled}}$ values a stacked record of relative abundance of hematite stained grains (%HSG) which are a tracer of Holocene drift ice in the North Atlantic (Bond et al. 2001) (peaks are numbered according to Bond et al. 1997) (Fig 4). During this period, there are five distinct increases in %HSG in the North Atlantic.

At the start of this period, $\delta^{18}\text{O}_{\text{modelled}}$ values decline to +27.3‰ at c. 11 300 cal yrs BP, concomitant with a small decline in silt contamination (Fig 4). The decline in the $\delta^{18}\text{O}_{\text{modelled}}$ record is coincident with IRD8, commonly known as the Preboreal Oscillation (PBO), a cool event associated with freshwater discharge (possibly from Lake Agassiz) into the North Atlantic (Fisher et al. 2002). Through intensification of the Siberian High, this cool event is likely to have resulted in the relative decline in proportion of rain-fed rivers flowing into Lake Baikal and relative increase in isotopically-lower rivers flowing into the lake from the north. As above, we acknowledge that further work is needed to improve the resolution of the $\delta^{18}\text{O}_{\text{modelled}}$ signal at this time. However, pollen data from Vydrino also suggests a short period of cooling (Demske et al. 2005), which may be responsible for very low numbers of diatom valves counted from the Buguldeika Saddle (Prokopenko et al. 2007). Quantitative climate reconstructions indicate that pollen-inferred annual precipitation declined until almost 11 000 cal yrs BP, together with a significant decline in temperature of the coldest month (but little change in temperature of the warmest month) (Tarasov et al. 2007; 2009). In the catchment of Lake Baikal taiga forest was still present, although steppe and tundra biomes were widespread (Tarasov et al. 2007).

$\delta^{18}\text{O}_{\text{modelled}}$ record subsequently rises to its highest values (+35.6‰) at 10 750 cal yrs BP and remain above +30‰ until c. 10 305 cal yrs BP. These high values are coincident with both low %HSG (Fig 4) (Bond et al. 1997) and highest July insolation values (Prokopenko et al. 2007). Errors in the isotopic data however are also very high, most likely due to the very high levels of detected silt contamination (Fig 3). These data suggest that there must have been significant hydrological input into Lake Baikal during the early Holocene from rivers with southerly catchments. Independent evidence suggests that this is quite likely; pollen-inferred annual precipitation is very high at this time in southern Lake Baikal (between 500 – 600 mm/yr) (Tarasov et al. 2009), as are GCM modelled annual mean freshwater fluxes (cm/day) and JJA relative humidity (%) (Bush 2005). It is not clear if the high levels of contamination are a direct result of increased

1
2
3 1 catchment in-wash, but diatom concentrations in several sites in the south basin of Lake
4 2 Baikal are also very low at this time (e.g. Bradbury et al. 1994; Prokopenko et al. 2007)
5 3 including the Vydrino shoulder (Morley 2005). Bradbury et al. (1994) suggest that
6 4 periods of low diatom concentration may be related to a decline in water transparency
7 5 caused by rivers bringing in terrigenous material, including fine clays and silts,
8 6 depressing photosynthetic activity. While we are not yet in a position to confirm that this
9 7 is the case, high levels of contamination (Fig 3) do not refute this hypothesis.
10 8

11 9 The greatest decline in the $\delta^{18}\text{O}_{\text{modelled}}$ record of +8‰ can be observed c. 10 275 – 10 030
12 10 cal yrs BP. This decline is synchronous with increased %HSG (IRD event no. 7) (Fig 4).
13 11 This cool event is seen in several archives from the e.g. North Atlantic sediments and
14 12 Greenland ice cores (c. 10 350 – 10 150 cal yr BP: see Björck et al. 2001 for a synthesis).
15 13 At this time, GCM modelled winter (DJF) temperatures showed a significant decline
16 14 (data from Bush 2005 and Prokopenko et al. 2007), while a decline in an index of warm
17 15 vegetation derived from Vydrino pollen confirms prevailing cooler conditions (Demske et
18 16 al. 2005).
19 17

20 18 $\delta^{18}\text{O}_{\text{modelled}}$ shows an overall rise to relatively high values between c. 10 000 – 8 560 cal
21 19 yrs BP. This isotopic increase occurs at the same time as a decline in %HSG (Fig 4), and
22 20 an increase in abundances of vegetation in the catchment indicative of warm, moist
23 21 climate (Demske et al. 2005; Tarasov et al. 2009). Thus, rivers such as the Selenga likely
24 22 increased in importance at this time. Several North Atlantic regions show a cool event
25 23 between c. 9 500 – 9 200 ka BP (IRD6), e.g. in Greenland ice cores (Rasmussen et al.
26 24 2007) and various European locations (e.g. von Grafenstein et al. 1999; McDermott et al.
27 25 2001), which Yu et al. (2010) attribute to freshwater outburst from Lake Superior in
28 26 North America. There are minor fluctuations in the isotope data (e.g. at c. 9 645 cal yrs
29 27 BP), which coincides with the start of increasing %HSG, but the decline at c. 9 200 cal
30 28 yrs BP is not significant and well within variation of the isotope data themselves. Any
31 29 impact of changes in the North Atlantic THC at this time on the composition of rivers
32 30 flowing into Lake Baikal does not therefore appear to be as great as previous events, e.g.
33 31 IRD 7 and 8).
34 32

35 33 There is a major decline in $\delta^{18}\text{O}_{\text{modelled}}$ record that starts c. 8 560 cal yrs BP, and reaches a
36 34 minimum c. 8 400 cal yrs BP. This decline once again coincides with a peak in %HSG
37 35 (Fig 4), IRD 5 (Bond et al. 2001). $\delta^{18}\text{O}_{\text{modelled}}$ values increase slightly again til c. 7 700
38 36 cal yrs BP, coinciding with a small decline in %HSG, before declining to a low value of
39 37 26.4‰ at c. 7 040 cal yrs BP, as %HSG increases to high abundances once more.
40 38 Therefore, isotopic evidence suggests an increase in input into Lake Baikal from
41 39 isotopically lower rivers with northern catchments, and a decline in rivers flowing in
42 40 from the south between c. 8 560 – 7 040 cal yrs BP. Work on a Selenga River Holocene
43 41 floodplain sequence at Burdukovo, which lies c. 30 km north of Ulan Ude, has revealed a
44 42 switch from alluvial to aeolian sedimentation processes sometime between c. 8 180 – 7
45 43 725 cal yrs BP (White & Bush 2010). This also implies that Selenga River levels were
46 44 low. Close inspection of other proxy records in the Lake Baikal region between c. 8 200 –
47 45 7 000 cal yrs BP show distinct low, modelled GCM summer temperatures (Bush 2005)
48 46 together with marked drops in diatom abundances and biogenic silica (Prokopenko et al.
49
50
51
52
53
54
55
56
57
58
59
60

1 2007). Moreover, vegetation indicative of humid conditions also decline (ibid.) as does
2 quantitative reconstruction of pollen-inferred annual precipitation (Tarasov et al. 2007),
3 although these records are in contrast of GCM modeled summer humidity which
4 increases at this time (Bush 2005).

5
6 Since 2001 a major international interdisciplinary programme (Baikal Archaeology
7 Project) has sought to characterise cultural dynamics among hunter-gatherer populations
8 around the Lake Baikal region during the mid Holocene (e.g. see Weber et al. 2002;
9 2010a). Results from this on-going research have redefined our understanding of hunter-
10 gatherer adaptive strategies during the Neolithic–Bronze Age, including aspects of culture
11 history, subsistence and diet, mobility patterns, genetic structure, and social and political
12 relations. Most of these new archaeological data have been derived from numerous well-
13 preserved formal cemetery contexts, which has allowed detailed analyses of human
14 skeletal remains. Focus has especially centered around a distinct biocultural discontinuity
15 between the early Neolithic Kitoi culture and the Serovo-Glazkovo cultures which
16 inhabited the area during the late Neolithic – early Bronze Age (Weber et al. 2002). Thus
17 by at least 7 000 cal yrs BP (i.e. middle Neolithic) there is a near absence of dated
18 archaeological cemetery evidence in the cis-Baikal region (Weber et al. 2005, 2010b). In
19 addition, clear shifts in subsistence adaptations (Katzenberg et al. 2010) and genetic
20 affiliation (Mooder et al. 2006; 2010) are also identified between these pre- and post-
21 hiatus groups. Reasons for this biological and cultural discontinuity are as yet uncertain,
22 although several hypotheses have been put forward, including climate and environmental
23 change (Weber et al. 2002; White and Bush 2010) and a decline in the use of formal
24 cemeteries due to a shift in foraging behaviour (Weber et al. 2005). Tarasov et al. (2007)
25 also reconstruct major changes in pollen-inferred climate variables between 7 200 – 6 000
26 cal yrs BP, most notably a decline in annual precipitation, concomitant with an increase in
27 steppe vegetation. It is not possible at this stage to conclude whether or not this shift to a
28 cooler, drier climate caused the observed hiatus between the Kitoi and Serovo-Glazkovo
29 cultures, but climate influence ought not yet be discounted.

30 31 4.1.3 Mid – late Holocene (7 000 cal yrs BP – present)

32
33 Northern hemisphere summer insolation levels were still relatively high during the mid-
34 Holocene, although North American ice sheets now had minimal impact on global
35 climates (Mayewski et al. 2004; Wanner et al. 2008). Cool events associated with Bond
36 cycles and increases in %HSG related to IRD4 to IRD0 were no longer associated with
37 melt-water outbursts but likely caused by a combination of factors (see Wanner et al.
38 2008 for a review). During this period, $\delta^{18}\text{O}_{\text{modelled}}$ values exhibit different relationships
39 the %HSG record in comparison to the similarities between the two records during the
40 early Holocene. For example, as %HSG values increase after c. 7 000 cal yrs BP,
41 $\delta^{18}\text{O}_{\text{modelled}}$ values also increase up to 5 890 cal yrs BP, at exactly the same time as
42 increasing contamination, which suggests increased flow of rivers such as the Selenga
43 and increased silt transport into the lake at the Vydrino site. This increase in $\delta^{18}\text{O}_{\text{modelled}}$ is
44 also at odds with the decline in pollen-inferred precipitation between c. 7 200 – 6 000 cal
45 yrs BP (Tarasov et al. 2007) and in water levels of the Mongolian lakes Hovsgol at c. 6
46 600 cal yrs BP (Dorofeyuk and Tarasov, 1998), and Telmen between c. 7 110 – 6 260 cal

1 yrs BP (Peck et al. 2002). Further afield, a shift to heavier $\delta^{18}\text{O}$ values from Dongge Cave (south China) between 7 200 – 6 600 cal yrs BP highlights a weakening monsoon system, linked to strengthened Siberian High (Dykoski et al. 2005). There is a significant decline in $\delta^{18}\text{O}_{\text{modelled}}$ record between c. 5 980 and 5 600 cal yrs BP which is coincident with IRD4 and also with very low values for GCM modelled annual mean freshwater flux and JJA relative humidity (Bush 2005). Thus, while the inferred decline in fluvial input into Lake Baikal from southerly rivers at c. 5 700 cal yrs BP does coincide with weak North Atlantic thermohaline, increasing $\delta^{18}\text{O}_{\text{modelled}}$ values just prior to this event are at odds with other proxy records. More work therefore needs to be done to better characterise changes in precipitation and river inflow into Lake Baikal at this time.

After c. 5 165 cal yrs BP there is a sustained period of declining $\delta^{18}\text{O}_{\text{modelled}}$ values, which spans IRD3, leading to the low $\delta^{18}\text{O}_{\text{modelled}}$ value of 26.3‰ at c. 3 330 cal yrs BP, which coincides with IRD2 (Bond et al. 2001) (Fig. 4). The decline in $\delta^{18}\text{O}_{\text{modelled}}$ values coincides with variability observed in other regional proxy records, including a major phase of reconstructed steppe vegetation around Lake Baikal between c. 5 700 – 3 800 cal yrs BP (Tarasov et al. 2007). Diatom and biogenic silica profiles from the Buguldeika Saddle also show marked declines at this time, consistent with GCM data (Colman et al. 1999; Prokopenko et al. 2007). In northern Mongolia, low lake levels at Gun Nuur were recorded at c. 3 540 cal yrs BP (Dorofeyuk and Tarasov 1998). Together these proxies suggest a significant period of aridity, although other lakes, such as Telmen suggest more humid conditions prevailed after 4 390 cal yrs BP (Peck et al. 2002). In central China, $\delta^{18}\text{O}$ from Dongge Cave record the longest and one of the most significant periods of aridity during the Holocene (Wang et al. 2005) between c. 4 500 – 4 000 cal yrs BP. This period also coincides with IRD event 3 (Bond et al. 2001) and the collapse of the Neolithic culture in China.

From c. 3 330 - 2 630 cal yrs BP the $\delta^{18}\text{O}_{\text{modelled}}$ record is very poorly resolved. However, between c. 2 630 til c. 2 060 cal yrs BP, $\delta^{18}\text{O}_{\text{modelled}}$ values are at their highest during the mid- late Holocene, indicative of major influence of isotopically higher rivers flowing into Lake Baikal due to a weak Siberian High. High $\delta^{18}\text{O}_{\text{modelled}}$ values occur at the same time as low %HSG, very low steppe biome scores and increasing pollen-inferred temperatures (Tarasov et al. 2007). This increase is also mirrored by an increase in biogenic silica from the Buguldeika core (Prokopenko et al. 2007). Modelled annual freshwater flux also is very high at this time (Bush 2005). Regional records also concur with increased effective moisture. For example, in Lake Telmen laminated sediments accumulated between 2 210 and 2 070 cal yrs BP during which time deep lake levels must have predominated (Peck et al. 2002) due to high precipitation over northern Mongolia. Further south, proxy evidence from the Chinese Guliya ice cores highlight a period of marked warm and moist conditions, indicative of a weakened Siberian High and strong summer Asian monsoon (Yang et al. 2004). Proxy evidence from a number of different sources therefore confirm widespread warm and wet climate in the Lake Baikal region, coincidental with strengthened North Atlantic THC (Bond et al. 2001).

$\delta^{18}\text{O}_{\text{modelled}}$ record for the late Holocene is unfortunately at a very low resolution, making any useful comparisons to the %HSG record problematic. Overall, $\delta^{18}\text{O}_{\text{modelled}}$ values do

1 decline towards the top of the record, coincident with declining biogenic silica
2 concentrations (Prokopenko et al. 2007) and a marked fall in GCM modelled summer
3 temperatures (Bush 2005). Low resolution $\delta^{18}\text{O}_{\text{diatom}}$ records from the north of Lake
4 Baikal also decline at this time, highlighting the wide spatial extent of this event
5 (Kalmychkov et al. 2007). A decline in effective moisture in northern Mongolia is also
6 apparent in the sediment records from Lake Telmen, resulting in, for example, a high-
7 stand terrace c. 1400 – 1260 cal yrs BP (Peck et al. 2002). Tree-ring data highlight a
8 series of severe droughts affecting northern Mongolia during the early 18th and 19th
9 centuries (Pederson et al. 2001). These observations are concurrent with the most recent
10 IRD events in the North Atlantic, including event 0, which is coeval with the Little Ice
11 Age. The drop in $\delta^{18}\text{O}_{\text{diatom}}$ values from c. 360 cal yrs BP might well be a response to a
12 cooler climate associated with the LIA, which has been shown to have had a major
13 impact on diatom communities close to Vydrino at this time (Mackay et al. 2005).

14 15 **6. Conclusions**

16
17 In this paper we present a new, recalculated mass-balanced model of $\delta^{18}\text{O}_{\text{diatom}}$ data for
18 the late glacial – Holocene period in Lake Baikal. The improvement over a previous
19 record has only been possible by accurately taking into account contaminants remaining
20 in purified diatom silica samples, using electron optical imaging and whole sample
21 geochemistry, as well as considering Al bound diatom concentrations. We interpret the
22 $\delta^{18}\text{O}_{\text{modelled}}$ record as a proxy for the composition of river flow into Lake Baikal, with
23 respect to the balance between rivers flowing into the lake with southern as opposed to
24 northern catchments. Changes in this record show, in general, very good correspondence
25 with proxy records of %HSG in the North Atlantic associated with enhanced meridional
26 circulation at least during the early to mid Holocene. Between c. 7 000 – 6 000 cal yrs BP,
27 increasing $\delta^{18}\text{O}_{\text{modelled}}$ values at odds with other proxy records in the region, and more
28 work over this time frame needs to be undertaken to investigate possible reasons for this
29 discrepancy.

30 31 **7. Acknowledgements**

32
33 Various funding sources have helped contribute to the production of data in this paper,
34 including EU FPV *Continent* project (Contract EVK2-2000-00057); NERC NIGL
35 (IP/635/0300); NERC PhD studentship to DWM (NER/S/A/2001/06430); Baikal
36 Archaeology Project, supported by the Major Collaborative Research Initiative (MCRI)
37 programme of the Social Sciences and Humanities Research Council of Canada; The
38 Royal Society through the UK BICER programme.

8. References

- Afanasjev AN. 1976. *The Water Resources and Water Balance of the Lake Baikal Basin* [in Russian]. Nauka, Novosibirsk.
- Bezrukova EV, Abzaeva AA, Letunova PP, Kulagina NV, Vershin KE, Belov AV, Orlova LA, Danko LV, Krapivina SM. 2005. Post-glacial history of Siberian spruce (*Picea obovata*) in the Lake Baikal area and the significance of this species as a paleo-environmental indicator. *Quaternary International* **136** : 47-57.
- Björck S, Muscheler R, Kromer B, Andresen CS, Heinemeier J, Johnsen SJ, Conley D, Koç N, Spurk M, Veski S. 2001. High-resolution analyses of an early Holocene climate event may imply decreased solar forcing as an important climate trigger. *Geology* **29** : 1107-1110.
- Blackwell, PG, Buck CE, Reimer PJ. 2006. Important features of the new radiocarbon calibration curves. *Quaternary Science Reviews* **25** : 408-413.
- Bond G, Showers W, Cheseby M, Lotti R, Almasi P, deMenocal P, Priore P, Cullen H, Hajdas I, Bonani G. 1997. A pervasive millennial scale cycle in North Atlantic Holocene and glacial climates. *Science* **278** : 1257-1256.
- Bond G, Kromer B, Beer J, Muscheler R, Evans M, Showers W, Hoffmann S, Lotti-Bond R, Hajdas I, Bonani G. 2001. Persistent solar influence on North Atlantic climate during the Holocene. *Science* **294** : 2130-2136.
- Bradbury JP, Bezrukova YeV, Chernyaeva GP, Colman SM, Khursevich G, King JW, Likoshway YeV. 1994. A synthesis of post-glacial diatom records from Lake Baikal. *Journal of Paleolimnology* **10** : 213-252.
- Brewer T, Leng M, Mackay AW, Lamb A, Tyler J, Marsh N. 2008. Unravelling contamination signals in biogenic silica oxygen isotope composition: the role of major and trace element geochemistry. *Journal of Quaternary Science* **23** : 365-374.
- Bronk Ramsey C. 2009. Bayesian analysis of radiocarbon dates. *Radiocarbon* **51** : 337-360.
- Bush ABG. 2005. CO₂/H₂O and orbitally driven climate variability over central Asia through the Holocene. *Quaternary International* **136** : 15-23.
- Campbell ID, Campbell C, Apps M, Rutter NW, Bush ABG. 1998. Late Holocene ~1500 yr climatic periodicities and their implications. *Geology* **26** : 471-473.
- Charlet F, Fagel N, De Batist M, Hauregard F, Minnebo B, Meischner D, SONIC Team. 2005. Sedimentary dynamics on isolated highs in Lake Baikal: evidence from detailed

- 1 high-resolution geophysical data and sediment cores. *Global and Planetary Change* **46** :
2 125-144.
- 3
4
5
6
7 4 Chebykin EP, Edgington DN, Grachev MA, Zzheleznyakova TO, Vorobyova SS,
8 5 Kulikova NS, Azarova IN, Khlystov OM, Goldberg EL. 2002. Abrupt increase in
9 6 precipitation and weathering of soils in East Siberia coincident with the end of the last
10 7 glaciation (15 cal kyr BP). *Earth and Planetary Science Letters* **200** : 167-175.
11 8
12 9 Colman SM, Peck JA, Hatton J, Karabanov EB, King JW. 1999. Biogenic silica records
13 10 from the BDP93 drill site and adjacent areas of the Selenga Delta, Lake Baikal, Siberia.
14 11 *Journal of Paleolimnology* **21** : 9-17.
15 12
16 13 deMenocal P, Ortiz J, Guilderson T, Sarnthein M. 2000. Coherent high and low latitude
17 14 climate variability during the Holocene warm period. *Science* **288** : 2198-2202.
18 15
19 16 Demske D, Heumann G, Granoszewski W, Nita M, Mamakowa K, Tarasov PE,
20 17 Oberhänsli H. 2005. Late glacial and Holocene vegetation and regional climate variability
21 18 evidenced in high-resolution pollen records from Lake Baikal. *Global & Planetary*
22 19 *Change* **46** : 255-279.
23 20
24 21 Dorofeyuk NI, Tarasov PE. 1998. Vegetation and lake levels in northern Mongolia during
25 22 the past 12500 years from palynological and diatom analyses. *Stratigraphy and Geologic*
26 23 *Correlation* **6** : 73-87.
27 24
28 25 Dykoski CA, Edwards RL, Cheng H, Yuan D, Cai Y, Zhang M, Lin Y, Qing J, An Z,
29 26 Revenaugh J. 2005. A high-resolution, absolute-dated Holocene and deglacial Asian
30 27 monsoon record from Dongge Cave, China. *Earth and Planetary Science Letters* **233** :
31 28 71-86.
32 29
33 30 Fisher TG, Smith DG, Andrews JT. 2002. Preboreal oscillation caused by a glacial Lake
34 31 Agassiz flood. *Quaternary Science Reviews* **21** : 873-878.
35 32
36 33 Grunert J, Lehmkuhl F, Walther M. 2000. Paleoclimatic evolution of the Uvs Nuur basin
37 34 and adjacent areas (Western Mongolia). *Quaternary International* **65-66** : 171-192.
38 35
39 36 Hampton SE, Izmet'eva LR, Moore MV, Katz SL, Dennis B, Silow EA. 2008. Sixty
40 37 years of environmental change in the world's largest freshwater lake—lake Baikal, Siberia.
41 38 *Global Change Biology* **14** : 1947-1958.
42 39
43 40 Heegaard E, Birks HJB, Telford RJ. 2005. Relationships between calibrated ages and
44 41 depth in stratigraphical sequences: as estimation procedure by mixed-effect regression.
45 42 *The Holocene* **15** : 612-618.
46 43
47 44 Heiri O, Tinner W, Lotter A. 2004. Evidence for cooler European summers during periods
48 45 of changing meltwater flux to the North Atlantic. *Proceedings of the National Academy of*
49 46 *Sciences* **101** : 15285-15288.
50
51
52
53
54
55
56
57
58
59
60

- 1
2
3
4 1
5 2 Hu, FS, Shemesh A. 2003. A biogenic-silica $\delta^{18}\text{O}$ record of climatic change during the
6 3 last glacial-interglacial transition in southwestern Alaska. *Quaternary Research* **59** : 379-
7 4 385.
8 5
9 6 Jones VJ, Leng MJ, Solovieva N, Sloane H, Tarasov P. 2004. Holocene climate of the
10 7 Kola Peninsula; evidence from the oxygen isotope record of diatom silica. *Quaternary*
11 8 *Science Reviews* **23** : 833-839.
12 9
13 10 Kalmychkov GV, Kuzmin MI, Pokrovskii BG, Kostrova SS. 2007. Oxygen isotopic
14 11 composition in diatom algae frustules from Lake Baikal sediments: annual mean
15 12 temperature variations during the last 40 ka. *Doklady Earth Sciences* **413** : 206-209.
16 13
17 14 Katzenberg MA, Bazaliiskii VI, Goriunova OI, Savel'ev NA, Weber AW. 2010. Diet
18 15 reconstruction and stable isotope ecology in the Lake Baikal region. In *Prehistoric*
19 16 *Hunter-Gatherers of the Baikal Region, Siberia: Bioarchaeological Studies of Past*
20 17 *Lifeways*, Weber AW, Katzenberg MA, Schurr TG (eds) University of Pennsylvania
21 18 Museum Press. in press.
22 19
23 20 Koning E, Gehlen M, Flank AM, Calas G, Epping E. 2007. Rapid post-mortem
24 21 incorporation of aluminum in diatom frustules: evidence from chemical and structural
25 22 analyses. *Marine Chemistry* **103** : 97–111.
26 23
27 24 Kozhova OM, Izmet'eva LR. 1998. *Lake Baikal: evolution and biodiversity*. Backhuys
28 25 Publishers: Leiden.
29 26
30 27 Kurita N, Yoshida N, Inoue G, Chayanova EA. 2004. Modern isotope climatology of
31 28 Russia: a first assessment. *Journal of Geophysical Research* **109** : D03102 15 pp.
32 29
33 30 Lamb AL, Brewer TS, Leng MJ, Sloane HJ, Lamb HF. 2007. A geochemical method for
34 31 removing the effect of tephra on lake diatom oxygen isotope records. *Journal of*
35 32 *Paleolimnology* **37** : 499-516.
36 33
37 34 Leng M, Barker P. 2006. A review of the oxygen isotope composition of lacustrine diatom
38 35 silica. *Earth Science Reviews* **75** : 5-27.
39 36
40 37 Leng MJ, Sloane H. 2008. Combined oxygen and silicon isotope analysis of biogenic
41 38 silica. *Journal of Quaternary Science* **23** : 3113-319.
42 39
43 40 Livingstone DM. 1999. Ice break-up on southern Lake Baikal and its relationship to local
44 41 and regional air temperatures in Siberia and to the North Atlantic Oscillation. *Limnology*
45 42 *& Oceanography* **44** : 1486-1497.
46 43
47 44 Lui X, Yanai M. 2002. Influence of Eurasian spring snow cover on Asian summer
48 45 rainfall. *International Journal of Climatology* **22** : 1075-1089.
49 46
50
51
52
53
54
55
56
57
58
59
60

- 1
2
3 1 Lydolph PE. 1977. *Eastern Siberia*. In *Climates of the Soviet Union. World Survey of*
4 2 *Climatology*, 7, Elsevier, pp 91-115.
5 3
6 4 Ma X, Yasunari T, Ohata T, Natsagdorj L, Davaa G, Oyunbaatar D. 2003. Hydrological
7 5 regime analysis of the Selenge River basin, Mongolia. *Hydrological Processes* 17 : 2929-
8 6 2945.
9 7
10 8 Mackay AW, Ryves DB, Battarbee RW, Flower RJ, Jewson D, Rioual PMJ, Sturm M.
11 9 2005. 1000 years of climate variability in central Asia: assessing the evidence using Lake
12 10 Baikal diatom assemblages and the application of a diatom-inferred model of snow
13 11 thickness. *Global & Planetary Change* 46 : 281-297.
14 12
15 13 Mackay AW, Karabanov E, Khursevich G, Leng M, Morley DW, Panizzo VN, Sloane HJ,
16 14 Williams D. 2008. Reconstructing hydrological variability in Lake Baikal during MIS 11:
17 15 an application of oxygen isotope analysis of diatom silica. *Journal of Quaternary Science*
18 16 23 : 365-374.
19 17
20 18 Mayewski PA, Rohling EE, Stager JC, Karlén W, Maasch KA, Meeker LD, Meyerson
21 19 EA, Gasse F, van Kreveld S, Holmgren K, Lee-Thorp J, Rosqvist G, Rack F, Staubwasser
22 20 M, Schneider RR, Steig EJ. 2004. Holocene climate variability. *Quaternary Research* 62 :
23 21 243-255.
24 22
25 23 McDermott F, Matthey DP, Hawkesworth CJ. 2001. Centennial scale Holocene climate
26 24 variability revealed by a high-resolution speleothems ¹⁸O record from S. W. Ireland.
27 25 *Science* 294 : 1328.
28 26
29 27 Mooder KP, Schurr TG, Bamforth FJ, Bazaliiski VI, Savel'ev NA. 2006. Population
30 28 affinities of Neolithic Siberians: a snapshot from prehistoric Lake Baikal. *American*
31 29 *Journal of Physical Anthropology* 129 : 349-61.
32 30
33 31 Mooder KP, Thomson TA, Weber AW, Bazaliiskii VI, Bamforth F. 2010. Uncovering the
34 32 genetic landscape of prehistoric Cis-Baikal. In *Prehistoric Hunter-Gatherers of the*
35 33 *Baikal Region, Siberia: Bioarchaeological Studies of Past Lifeways*, Weber AW,
36 34 Katzenberg MA, Schurr TG (eds) University of Pennsylvania Museum Press. 107-120.
37 35
38 36 Morley DW. 2005. *Reconstructing past climate variability in continental Eurasia*.
39 37 Unpublished PhD Thesis, University of London.
40 38
41 39 Morley DW, Leng MJ, Mackay AW, Sloane H, Rioual P, Battarbee RW. 2004. Cleaning
42 40 of lake sediment samples for diatom oxygen isotope analysis. *Journal of Paleolimnology*
43 41 31 : 391-401.
44 42
45 43 Morley DW, Leng MJ, Mackay AW, Sloane HJ. 2005. Late Glacial and Holocene
46 44 atmospheric circulation change in the Lake Baikal region documented by oxygen isotopes
47 45 from diatom biogenic silica. *Global & Planetary Change* 46 : 221-233.
48 46
49
50
51
52
53
54
55
56
57
58
59
60

- 1
2
3 1 Murton JB, Bateman MD, Dallimore SR, Teller JT, Yang Z. 2010. Identification of
4 2 Younger Dryas outburst flood path from Lake Agassiz to the Arctic Ocean. *Nature* **464** :
5 3 740-743.
6 4
7 4
8 5 Nesje A, Jansen E, Birks HJB, Bjune AE, Bakke J, Andersson C, Dahl SO, Kristensen
9 6 DK, Lauritzen S-E, Lie Ø, Risebrobakken B, Svendsen I. 2005. Holocene climate
10 7 variability in the northern North Atlantic region: a review of terrestrial and marine
11 8 evidence. In: *The Nordic Seas: An integrated perspective, Geophysical Monograph Series*
12 9 **158** : 289-322.
13 10
14 11 Numaguti A. 1999. Origin and recycling processes of precipitating water over the
15 12 Eurasian continent: experiments using an atmospheric general circulation model. *Journal*
16 13 *of Geophysical Research* **104** : 1957-1972.
17 14
18 15 Peck JA, Khosbayar P, Fowell SJ, Pearce RB, Ariunbileg S, Hansen BCS, Soninkhishig
19 16 N. 2002. Mid to Late Holocene climate change in north central Mongolia as recorded in
20 17 the sediments of Lake Telmen. *Palaeogeography, Palaeoclimatology, Palaeoecology* **183**
21 18 : 135-153.
22 19
23 20 Pederson N, Jacoby GC, D'Arrigo RD, Cook ER, Buckley BM. 2001.
24 21 Hydrometeorological reconstructions for northeastern Mongolia derived from tree rings:
25 22 1651-1995. *Journal of Climate* **14** : 872-881.
26 23
27 24 Piotrowska N, Bluszcz A, Demske D, Granoszewski W, Heumann G. 2004. Extraction
28 25 and AMS radiocarbon dating of pollen from Lake Baikal sediments. *Radiocarbon* **46** :
29 26 181-187.
30 27
31 28 Prokopenko AA, Kuzmin MI, Williams DF, Gelety VF, Kalmychkov GV, Gvozdkov AN,
32 29 Solotchin PA. 2005. Basin-wide sedimentation changes and deglacial lake-level rise in
33 30 the Hovsgol basin, NW Mongolia. *Quaternary International* **136** : 59-69.
34 31
35 32 Prokopenko AA, Khursevich GK, Bezrukova EV, Kuzmin MI, Boes X, Williams DF,
36 33 Fedenya SA, Kulagina NV, Letunova PP, Abzaeva AA. 2007. Paleoenvironmental proxy
37 34 records from Lake Hovsgol, Mongolia, and a synthesis of Holocene climate change in the
38 35 Lake Baikal watershed. *Quaternary Research* **68** : 2-17.
39 36
40 37 Prokopenko AA, Kuzmin MI, Li H-C, Woo K-S, Catto NR. 2009. Lake Hovsgol basin as
41 38 a new study site for long continental paleoclimate records in continental interior Asia:
42 39 general context and current status. *Quaternary International* **205** : 1-11.
43 40
44 41 Rasmussen DO, Andersen KK, Svensson AM, Steffensen JP, Vinther BM, Clausen HB,
45 42 Siggaard-Andersen M-L, Johnsen SJ, Larsen LB, Dahl-Jensen D, Bigler M, Rothlisberger
46 43 R, Fischer H, Goto-Azuma K, Hansson ME, Ruth U. 2006. A new Greenland ice core
47 44 chronology for the last glacial termination. *Journal of Geophysical Research* **111** : 1 of
48 45 16.
49 46
50
51
52
53
54
55
56
57
58
59
60

- 1 Rasmussen SO, Vinther BM, Clausen HB, Andersen KK. 2007. Early Holocene climate
2 oscillations recorded in three Greenland ice cores. *Quaternary Science Reviews* **26** :
3 1907–14.
- 4
5 Reimer PJ, Baillie MGL, Bard E, Bayliss A, Beck JW, Bertrand CJH, Blackwell PG,
6 Buck CE, Burr GS, Cutler KB, Damon PE, Edwards RL, Fairbanks RG, Friedrich M,
7 Guilderson TP, Hogg AG, Hughen KA, Kromer B, McCormac G, Manning S, Ramsey
8 CB, Reimer RW, Remmele S, Southon JR, Stuiver M, Talamo S, Taylor FW, Van der
9 Plicht J, Weyhenmeyer CE. 2004. IntCal04 Terrestrial Radiocarbon Age Calibration, 0–
10 26 Cal Kyr BP. *Radiocarbon* **46** : 1029-1058.
- 11
12 Rosqvist G, Jonsson C, Yam R, Karlén W, Shemesh A. 2004. Diatom oxygen isotopes in
13 pro-glacial lake sediments from northern Sweden: a 5000 year record of atmospheric
14 circulation. *Quaternary Science Reviews* **23** : 851-859.
- 15
16 Sato T, Tsujimura M, Yamanaka T, Iwasaki H, Sugimoto A, Sugita M, Kimura F, Davaa
17 G, Oyunbaatar D. 2007. Water sources in semi-arid Northeast Asia as revealed by field
18 observations and isotope transport model. *Journal of Geophysical Research- Atmospheres*
19 **112** : D17112.
- 20
21 Seal RR, Shanks WC. 1998. Oxygen and hydrogen isotope systematics of Lake Baikal,
22 Siberia: implications for palaeoclimate studies. *Limnology & Oceanography* **43** : 1251-
23 1261.
- 24
25 Shemesh A, Rosqvist G, Rietti-Shati M, Rubensdotter L, Bigler C, Yam R, Karlén W.
26 2001. Holocene climatic change in Swedish Lapland inferred from an oxygen-isotope
27 record of lacustrine biogenic silica. *The Holocene* **11** : 447-454.
- 28
29 Shimaraev MN, Verbolov VI, Granin NG, Sherstyankin PP. 1994. *Physical limnology of*
30 *Lake Baikal: a review*. BICER : Irkutsk-Okayama.
- 31
32 Soma Y, Tani Y, Soma M, Mitake H, Kurihara R, Hashimoto S, Watanabe T, Nakamura
33 T. 2007. Sedimentary steryl chlorin esters (SCEs) and other photosynthetic pigments as
34 indicators of palaeolimnological change over the last 28,000 years from the Buguldeika
35 Saddle of Lake Baikal. *Journal of Paleolimnology* **37** : 163-175.
- 36
37 Stuiver M, Grootes PM, Braziunas TF. 1995. The GISP2 $\delta^{18}\text{O}$ climatic record of the past
38 16,500 years and the role of the sun, ocean, and volcanoes. *Quaternary Research* **44** :
39 341–354.
- 40
41 Swann GEA. in press. A comparison of the Si/Al and Si/time wet-alkaline digestion
42 methods for measurement of biogenic silica in lake sediments. *Journal of Paleolimnology*
43
- 44 Swann GEA, Leng MJ. 2009. A review of diatom ^{18}O in palaeoceanography. *Quaternary*
45 *Science Reviews* **28** : 384-398.
- 46

- 1
2
3 1 Tarasov L, Peltier WR. 2005. Arctic freshwater forcing of the Younger Dryas cold
4 2 reversal. *Nature* **435** : 662-665.
5 3
6 4 Tarasov P, Bezrukova E, Karabanov E, Nakagawa T, Wagner M, Kulagina N, Letunova P,
7 5 Abzaeva A, Granoszewski W, Riedal F. 2007. Vegetation and climate dynamics during
8 6 the Holocene and Eemian interglacials derived from Lake Baikal pollen records.
9 7 *Palaeogeography, Palaeoclimatology, Palaeoecology* **252** : 440-457.
10 8
11 9 Tarasov PE, Bezrukova EV, Krivonogov SK. 2009. Late Glacial and Holocene changes in
12 10 vegetation cover and climate in southern Siberia derived from a 15 kyr long pollen record
13 11 from Lake Kotokel. *Climate of the Past Discussions* **5** : 127-151.
14 12
15 13 Todd MC, Mackay AW. 2003. Large-scale climate controls on Lake Baikal ice cover.
16 14 *Journal of Climate* **16** : 3186-3199.
17 15
18 16 von Grafenstein U, Erlenkeuser H, Brauer A, Jouzel J, Johnsen SJ. 1999. A mid-European
19 17 decadal isotope-climate record from 15,500 to 5000 years BP. *Science* **284** : 1654– 1657.
20 18
21 19 Wang Y, Cheng H, Edwards RL, He Y, Kong X, An Z, Wu J, Kelly MJ, Dykoski CA, Li
22 20 X. 2005. The Holocene Asian monsoon: links to solar changes and North Atlantic
23 21 climate. *Science* **308** : 854-857.
24 22
25 23 Wanner H, Beer J, Bütikofer J, Crowley TJ, Cubasch U, Flückiger J, Goosse H, Grosjean
26 24 M, Joos F, Kaplan JO, Küttel M, Müller SA, Prentice C, Solomina O, Stocker TF, Tarasov
27 25 P, Wagner M, Widmann M. 2008. Mid- to Late Holocene climate change: an overview.
28 26 *Quaternary Science Reviews* **27** : 1791-1828.
29 27
30 28 Watanabe T, Nakamura T, Watanabe Nara F, Kakegawa T, Nishimura M, Shimokawara
31 29 M, Matsunaka T, Senda R, Kawai T. 2009. A new age model for the sediment cores from
32 30 Academician ridge (Lake Baikal) based on high-time-resolution AMS ¹⁴C data sets over
33 31 the last 30 kyr: paleoclimatic and environmental implications. *Earth and Planetary
34 32 Science Letters* **286** : 347-354.
35 33
36 34 Weber AW, Link DW, Katzenberg MA. 2002. Hunter-gather culture change and
37 35 continuity in the middle Holocene of the cis-Baikal, Siberia. *Journal of Anthropological
38 36 Archaeology* **21** : 230-299.
39 37
40 38 Weber AW, McKenzie HG, Beukens R. 2005. Evaluation of radiocarbon dates from a
41 39 Middle Holocene hunter-gatherer cemetery Khuzhir-Nuge XIV, Lake Baikal, Siberia.
42 40 *Journal of Archaeological Science* **32** : 1481–1500.
43 41
44 42 Weber AW, Katzenberg MA, Schurr TG. Eds. 2010a. *Prehistoric Hunter-Gatherers of the
45 43 Baikal Region, Siberia: Bioarchaeological Studies of Past Lifestyles*. Pp xv-xx.
46 44
47 45 Weber AW, McKenzie HG, Beukens R. 2010b. Radiocarbon dating of Middle Holocene
48 46 culture history in the Cis-Baikal. In *Prehistoric Hunter-Gatherers of the Baikal Region*,

- 1
2
3 1 *Siberia: Bioarchaeological Studies of Past Lifeways*, Weber AW, Katzenberg MA, Schurr
4 2 TG (eds) University of Pennsylvania Museum Press. 27-50.
5 3
6 4 White D, Bush ABG. 2010. Holocene climate, environmental variability and Neolithic
7 5 biocultural discontinuity in the Lake Baikal region. In *Prehistoric Hunter-Gatherers of*
8 6 *the Baikal Region, Siberia: Bioarchaeological Studies of Past Lifeways*, Weber AW,
9 7 Katzenberg MA, Schurr TG (eds) University of Pennsylvania Museum Press. 1-26.
10 8
11 9 Yang B, Braeuning A, Shi Y, Chen F. 2004. Evidence for a late Holocene warm and
12 10 humid climate period and environmental characteristics in the arid zones of northwest
13 11 China during 2.2 ~ 1.8 kyr BP. *Journal of Geophysical Research* **109** : D02105.
14 12
15 13 Yu S-Y, Colman SM, Lowell TV, Milne GA, Fisher TG, Breckenridge A, Boyd M, Teller
16 14 JT. 2010. Freshwater outburst from Lake Superior as a trigger for the cold event 9300
17 15 years ago. *Science* **328** : 1262-1266.
18
19
20
21
22
23
24
25
26
27
28
29
30
31
32
33
34
35
36
37
38
39
40
41
42
43
44
45
46
47
48
49
50
51
52
53
54
55
56
57
58
59
60

1
2
3
4
5
6
7
8
9
10
11
12
13
14
15
16
17
18
19
20
21
22
23
24
25
26
27
28
29
30
31
32
33
34
35
36
37
38
39
40
41
42
43
44
45
46
47
48
49
50
51
52
53
54
55
56
57
58
59
60

Figure legends

1
2
3
4
5
6
7
8
9
10
11
12
13
14
15
16
17
18
19
20
21
22
23
24
25
26
27
28
29
30
31
32
33
34
35
36
37
38
39
40
41
42
43
44
45
46
47
48
49
50
51
52
53
54
55
56
57
58
59
60

Fig. 1. Location of Lake Baikal, its three largest tributaries (Selenga, Upper Angara and Barguzin rivers), its outflow (Angara River) and coring location at the Vydrino Shoulder.

Fig. 2. Age-depth model based on calibrated radiocarbon AMS dates for composite cores from Vydrino Shoulder (CON01-605-5 and CON01-605-3) constructed using a generalised mixed-effect regression based on a generalised additive model (GAM) with constant variance (Heegaard et al. 2005). Grey-shaded area represents 95% confidence intervals of modelled ages (black line), black diamonds – midpoints of calibrated age ranges.

Fig 3. Comparative plots showing $\delta^{18}\text{O}_{\text{diatom}}$ (open circles) (Morley et al. 2005) and $\delta^{18}\text{O}_{\text{modelled}}$ (closed black squares; this study) profiles. % silt contamination is calculated from the amount of Al_2O_3 in individual samples. See text for details.

Fig. 4. Stratigraphic profiles of proxies highlighted in the text, plotted on a radiocarbon calibrated age scale. $\delta^{18}\text{O}_{\text{modelled}}$ profile with associated errors linked to mass-balancing isotope measurements (see text for details); four stacked records of relative abundance of hematite stained grains (%HSG) in North Atlantic sediments indicative of ice rafted debris events (see Bond et al. 2001 for full details). IRD numbers are according to those originally given in Bond et al. (1997). YD (Younger Dryas) and IACP (intra-Allerød cold period) are also highlighted.

Table 1. Sediment cores collected from the Vydrino Shoulder, Lake Baikal

Core code	Type	Lat.	Long.	Water depth	Core length
CON01-605-3	piston	51.5849	104.8548	675 m	10.45 m
CON01-605-5	box	51.5835	104.8518	665 m	2.50 m

1
2
3
4
5
6
7
8
9
10
11
12
13
14
15
16
17
18
19
20
21
22
23
24
25
26
27
28
29
30
31
32
33
34
35
36
37
38
39
40
41
42
43
44
45
46
47
48
49
50
51
52
53
54
55
56
57
58
59
60

1

Table 2. Radiocarbon dating profile from Vydrino location in the south basin of Lake Baikal. AMS dates from pollen extracts were calibrated using Oxcal4.1 program and IntCal04 radiocarbon calibration curve (Reimer et al. 2004). Depth interval and mid-depth are the original depths of samples from either the box core (CON01-605-5) or the piston core (CON01-605-3); sample thickness is the thickness of sediment samples processed to obtain pollen and spore concentrates; corrected depth values are those determined once cores have been spliced together and missing core tops taken into account; pollen purity (%) was estimated on the basis of particle counts; age ^{14}C BP are uncalibrated radiocarbon ages; unc is the laboratory uncertainty associated with each ^{14}C age; calibrated age range is limited by younger and older boundaries for 95.4% probability distribution of calendar age obtained after calibration; mid-point 94.5% is the central point estimation of the calibrated age range, and +/- is half of this range.

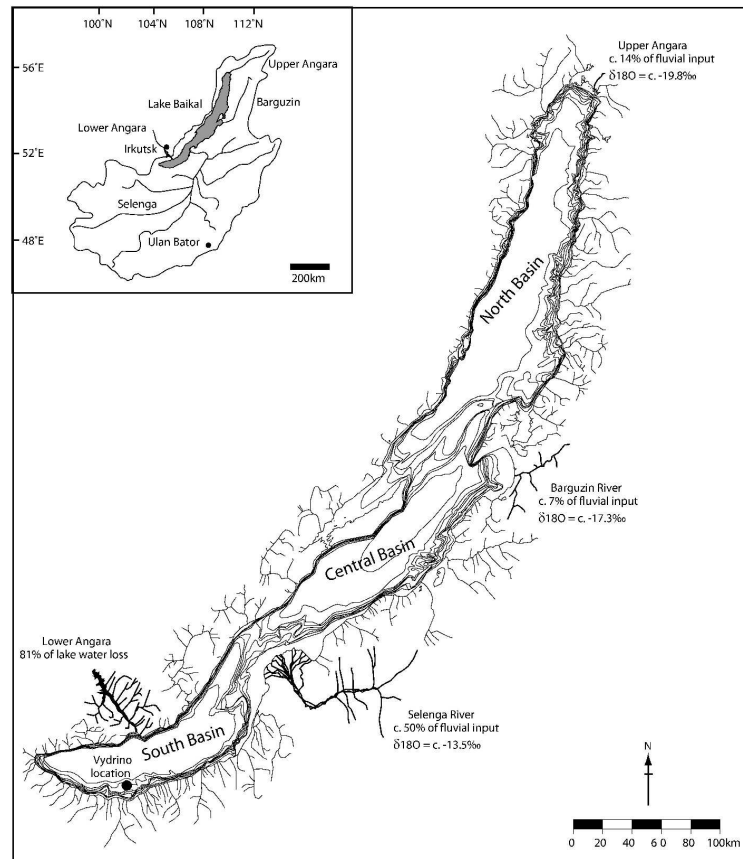
14

Table 3. Comparison of summary $\delta^{18}\text{O}$ between datasets presented by Morley et al. (2005) and this study.

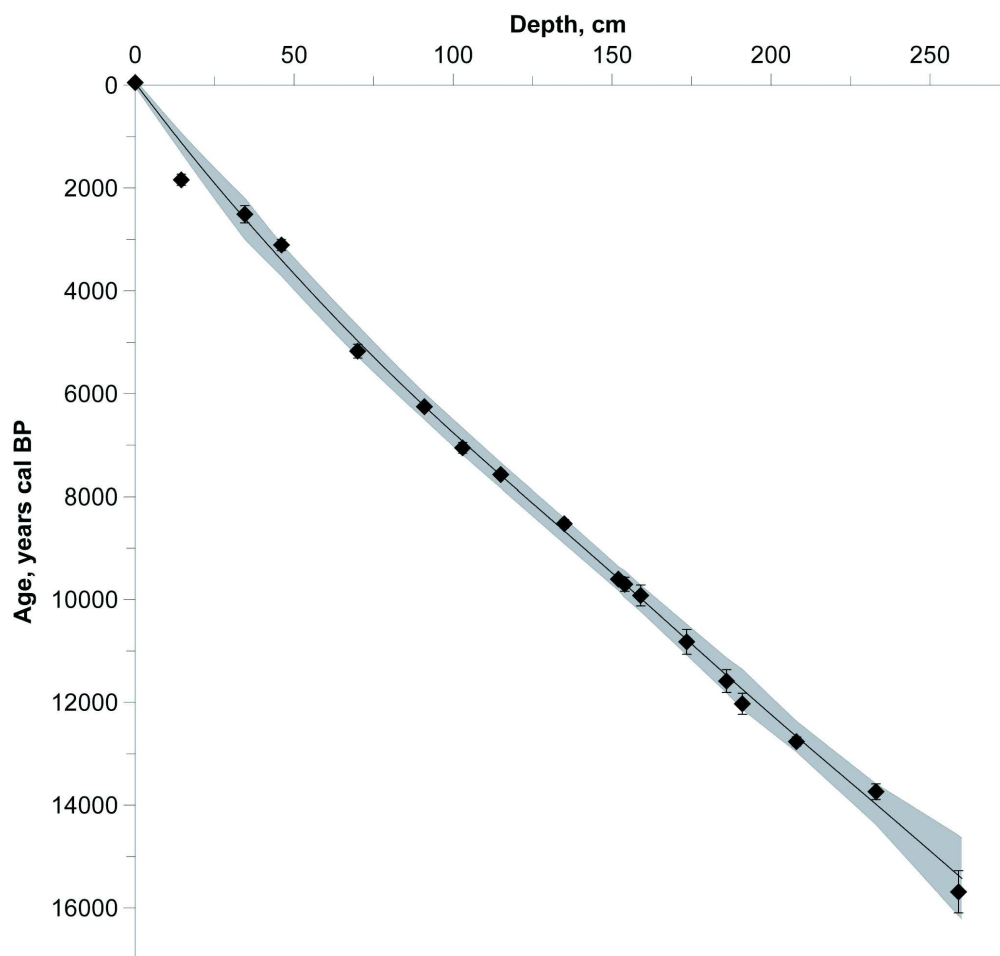
	Lowest (‰)	highest (‰)	range (‰)	mean (‰)	No of samples
Morley et al. (2005)	14.4	29.4	15.0	23.6 +/- 3.82	130
This study	23.9	35.6	11.7	28.7 +/- 2.15	55

Table 2

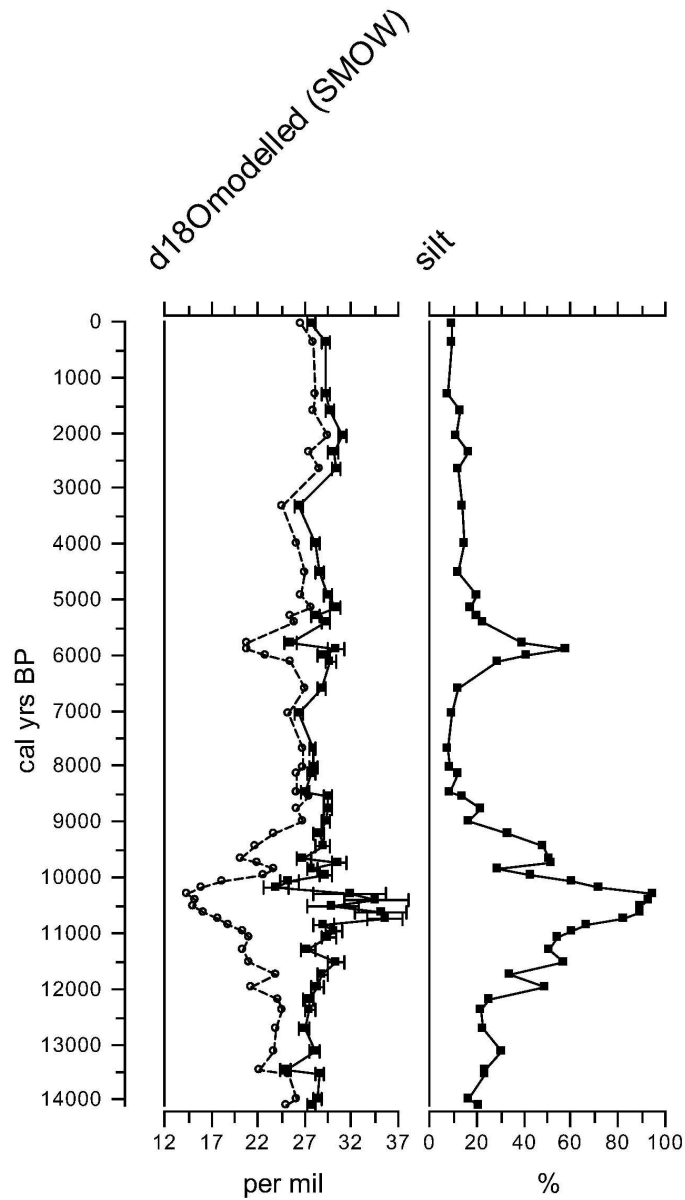
Core	Core code	Depth interval	Mid-depth	Sample thickness, cm	Corrected depth, cm	Pollen purity (%)	Age ¹⁴ C BP	unc	Calibrated age range, 95.4% probability
Box	LBB-AMS-1	0 4	2	4	14.5	90	1950	35	1950 17
Box	LBB-AMS-2	20 24	22	4	34.5	95	2375	25	2680 23
Box	LBB-AMS-3	32 35	33.5	3	46	95	2945	30	3215 30
Box	LBB-AMS-4	56 59	57.5	3	70	95	4530	40	5310 50
Box	LBB-AMS-5	77 80	78.5	3	91	95	5455	35	6305 62
Box	LBB-AMS-6	89 92	90.5	3	103	90	6170	40	7160 69
Box	LBB-AMS-7	101 104	102.5	3	115	85	6700	40	7650 75
Box	LBB-AMS-8	121 124	122.5	3	135	85	7760	40	8605 84
Box	LBB-AMS-9	138 141	139.5	3	152	90	8620	40	9680 95
Piston	LBF-AMS-11a	12 18	15	6	154	n.d.	8810	50	9840 95
Box	LBB-AMS-10	145 148	146.5	3	159	90	8750	50	10120 97
Box	LBB-AMS-11	159 163	161	4	173.5	90	9470	50	11060 105
Box	LBB-AMS-12	171.5 175.5	173.5	4	186	80	10030	50	11810 113
Piston	LBF-AMS-12a	48 56	52	8	191	n.d.	10340	60	12230 118
Piston	LBF-AMS-13	65 73	69	8	208	n.d.	10730	60	12850 123
Piston	LBF-AMS-14	90 98	94	8	233	n.d.	11820	70	13890 133
Piston	LBF-AMS-15	116 124	120	8	259	n.d.	13340	130	16090 152



Location of Lake Baikal, its three largest tributaries (Selenga, Upper Angara and Barguzin rivers), its outflow (Angara River) and coring location at the Vydrino Shoulder.
201x288mm (600 x 600 DPI)



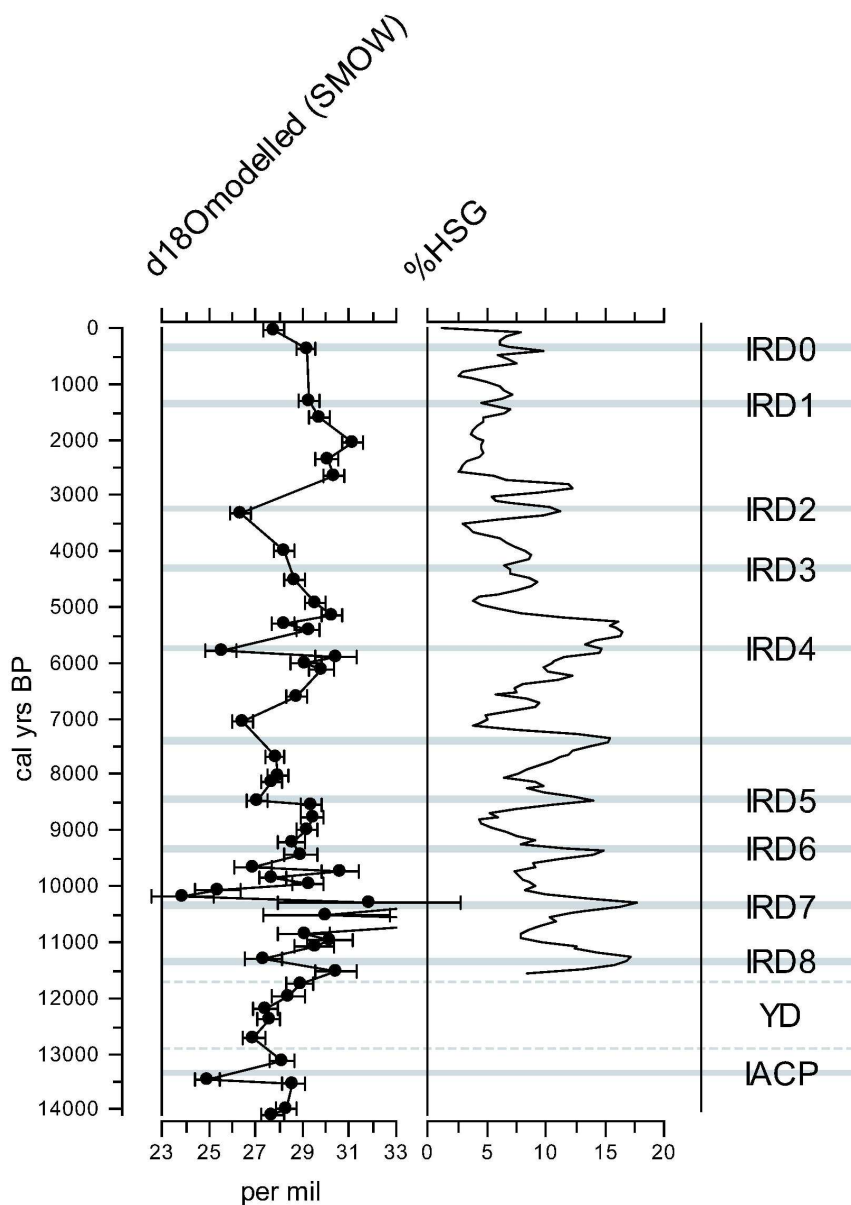
Age-depth model based on calibrated radiocarbon AMS dates for composite cores from Vydrino Shoulder (CON01-605-5 and CON01-605-3) constructed using a generalised mixed-effect regression based on a generalised additive model (GAM) with constant variance (Heegaard et al. 2005). Grey-shaded area represents 95% confidence intervals of modelled ages (black line), black diamonds – midpoints of calibrated age ranges
174x165mm (600 x 600 DPI)



Comparative plots showing $\delta^{18}\text{O}_{\text{diatom}}$ (open circles) (Morley et al. 2005) and $\delta^{18}\text{O}_{\text{modelled}}$ (closed black squares; this study) profiles. % silt contamination is calculated from the amount of Al_2O_3 in individual samples. See text for details.

108x192mm (600 x 600 DPI)

1
2
3
4
5
6
7
8
9
10
11
12
13
14
15
16
17
18
19
20
21
22
23
24
25
26
27
28
29
30
31
32
33
34
35
36
37
38
39
40
41
42
43
44
45
46
47
48
49
50
51
52
53
54
55
56
57
58
59
60



Stratigraphic profiles of proxies highlighted in the text, plotted on a radiocarbon calibrated age scale. $\delta^{18}O_{\text{modelled}}$ profile with associated errors linked to mass-balancing isotope measurements (see text for details); four stacked records of relative abundance of hematite stained grains (%HSG) in North Atlantic sediments indicative of ice rafted debris events (see Bond et al. 2001 for full details). IRD numbers are according to those originally given in Bond et al. (1997). YD (Younger Dryas) and IACP (intra-Allerød cold period) are also highlighted.
136x192mm (600 x 600 DPI)